Since January 2020 Elsevier has created a COVID-19 resource centre with free information in English and Mandarin on the novel coronavirus COVID-19. The COVID-19 resource centre is hosted on Elsevier Connect, the company's public news and information website.
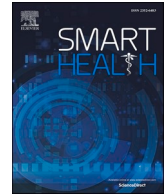
Wi-COVID: A COVID-19 symptom detection and patient monitoring framework using WiFi

Fangyu Li [a],[*],[1], Maria Valero [b],[1], Hossain Shahriar [b], Rumi Ahmed Khan [c],[d], Sheikh Iqbal Ahamed [e]

[a] *Department of Electrical and Computer Engineering, Kennesaw State University, United States*
[b] *Department of Information Technology, Kennesaw State University, United States*
[c] *Pulmonary Critical Care Medicine, Orlando Health, United States*
[d] *College of Medicine, University of Central Florida, United States*
[e] *Department of Computer Science, Marquette University, United States*

ARTICLE INFO

Keywords:
COVID-19
IoT
WiFi signals
End-to-end system
Respiratory rate

ABSTRACT

The current SARS-CoV-2, better know as COVID-19, has emerged as a serious pandemic with life-threatening clinical manifestations and a high mortality rate. One of the major complications of this disease is the rapid and dangerous pulmonary deterioration that can lead to critical pneumonia conditions, resulting in death. The current healthcare system around the world faces the potential problem of lacking resources to assist a large number of patients at the same time; then, the non-critical patients are mostly referred to perform self-isolation/quarantine at home. This pandemic has placed new demands on the *health systems world*, asking for novel, rapid and secure ways to monitor patients in order to detect and quickly report patient's symptoms to the healthcare provider, even if they are not in the hospital. While tremendous efforts have been done to develop technologies to detect the virus, create the vaccine, and stop the spread of the disease, it is also important to develop IoT technologies that can help track and monitor diagnosed COVID-19 patients from their homes. In this paper, we explore the possibility of monitoring respiration rates (RR) of COVID-19 patients using a widely-available technology at home – WiFi. Using the at-home WiFi signals, we propose Wi-COVID, a non-invasive and non-wearable technology to monitor the patient and track RR for the healthcare provider. We first introduce the currently available applications that can be done using WiFi signals. Then, we propose the framework scheme for an end-to-end non-invasive monitoring platform of the COVID-19 patients using WiFi. Finally, we present some preliminary results of the proposed framework. We envision the proposed platform as a life-changing technology that leverages WiFi technology as a non-wearable and non-invasive way to monitor COVID-19 patients at home.

1. Introduction

Coronavirus is a large family of viruses that can infect people and spread among humans in many forms such as with MERS-CoV,

* Corresponding author.
E-mail addresses: fli6@kennesaw.com (F. Li), mvalero2@kennesaw.edu (M. Valero), hshahria@kennesaw.edu (H. Shahriar), Rumi.Khan@orlandohealth.com (R.A. Khan), sheikh.ahamed@mu.edu (S.I. Ahamed).
[1] Both authors contributed equally to this work.

SARS-CoV, and now with the new virus SARS-CoV-2 (COVID-19) (C and Coronavirus Disease, 2020a). The clinical spectrum of COVID-19 infection appears to be wide, encompassing asymptomatic infection, mild upper respiratory tract illness, and severe viral pneumonia with respiratory failure and even death (Zhou et al. Gu). Pulmonary function, such as respiratory rate (RR), testing (Pulmonary Function Labora) is a way to measure the COVID-19 influences. Investigating the RR pattern and its relationship with COVID-19 symptoms is a hot topic nowadays (Ross, 2020). RR is the number of breaths a person takes per minute, which is usually measured when a person is at rest. RR simply involves counting the number of breaths for 1 min based on how many times the chest rises. RR may increase with fever, illness, and other medical conditions. For COVID-19 cases, RR is important to determine the pulmonary activity of the patients as abnormal measurements may indicate patient deterioration (Tenhunen, Elomaa, Sistonen, Rauhala, & Himanen, 2013).

Measuring RR usually involves the expertise of a health practitioner, so it is usually performed in the hospital. However, due to the clinical emergency caused by COVID-19, the RR and pulmonary function analysis of the diagnosed individuals increases the risk of contagious. The majority of patients do not present pulmonary distress initially, and healthcare providers have to make the difficult decision to send these patients back home and hope for their ability to engage in self-monitoring. According to the Center for Disease Control and Prevention (CDC), some patients with initial mild clinical presentation may worsen in the second week of illness (C and Coronavirus Disease, 2020a; Huang et al., 2020). Thus, patients whose pulmonary functions and RR have not been compromised and do not require hospitalizations should be monitored using tele-medicine tools while in self-isolation (Humphreys et al. Pantilat). Because of the high risk of diagnosed patients to develop severe respiratory distress, real-time RR monitoring of these patients is desirable. Even the Food and Drug Administration (FDA) has allowed the use of devices to monitor the patients vital signs remotely (O. o. t. Commissioner and Co, 2020). Unfortunately, there are limited tools available for real-time at-home monitoring, and mostly of them requires the use of wearable devices (e.g. watch, cuff, belt, etc.) or invasive technologies (like cameras).

To avoid the inconvenience of using wearable and invasive devices to monitoring vital signs, some contact-free technologies have been proposed. The advantages of contact-free sensing include continuous monitoring even during the night. The patient does not need to be aware of the device itself during sleep, where wearable devices can be a disruption. Most of monitoring contact-free technologies are based on force sensors (Alaziz et al., 2016), load cells (Adami, Hayes, Pavel, & Singer, 2006), multi-channel infrared sensor-arrays (Brser, Kerekes, Winter, & Leonhardt, 2012), pressure sensors (Ni, Abdulrazak, Zhang, & Wu, 2010), vibration sensors (Clemente, Valero, Li, Wang, & Song, 2020), and ratio frequency (Chen et al., 2017). Among them, one of the most interesting technologies is ratio frequency (RF) because this technology leverages the propagation of electromagnetic (EM) waves that can be extracted from the WiFi technology that almost everyone has at home. Nevertheless, none of the current approaches using WiFi for RR estimation includes a complete framework to analyze the patient in real-time and transfer the information to a healthcare practitioner for immediate response.

In this paper, we explore the possibility of monitoring RR on COVID-19 patients using a non-invasive, real-time and at-home technology. We propose Wi-COVID, a framework that uses the available WiFi signals generated by common-used equipment at home to monitor COVID-19 patients. Furthermore, using the at-home WiFi signals, we propose a non-invasive and non-wearable technology to monitor the patient and report the RR to the healthcare provider in real time. The proposed end-to-end framework includes: i) a platform for detecting and estimating RR using only information of the WiFi signal at home; and ii) a end-to-end system design for tracking real-time patient's RRs for the healthcare provider. We summarize our contributions as follows:

1. We provide a comprehensive review of the current WiFi-based available technology for monitoring vital signs and people's activities that can provide a novel approach to monitor patients.
2. We explore the possibility of using the WiFi-based technology to monitor diagnosed COVID-19 patients who are performing self-isolation in real-time.
3. We present preliminary results of the effectiveness of using WiFi-based information to extract RR and transmit the information to healthcare providers.
4. We propose an end-to-end free infrastructure framework (Wi-COVID) for healthcare monitoring during pandemics as it is built upon the existing WiFi networks available indoor.

The remainder of this paper is organized as follows. First, we discuss different approaches for WiFi monitoring in Section 2. Then, we introduce the proposed Wi-COVID framework in Section 3. The design of the WiFi-based system is represented in Section 4. We demonstrate preliminary results in Section 5.2. In Section 6, we describe the potential future directions. Finally, we draw our conclusions in Section 7.

2. WiFi-based monitoring approaches

Non-invasive or unobtrusive sensing is particularly interesting for the acquisition of health-related information. Among the various approaches to measuring health information, especially vital signs and activity recognition, wireless sensing has received increasing attention because of the ubiquitous deployment of wireless radio devices. In general, the WiFi signals are collected from the wireless WiFi module board using certain API software (Gringoli, Schulz, Link, & Hollick, 2019).

WiFi-based acquisition and recognition techniques usually include one of three approaches: the use of radio signal strength (RSS), the use of channel state information (CSI), or the use of Frequency Modulated Continuous Wave (FMCW) information. RSS provides coarse-grained information about communication links (Yang, Zhou, & Liu, 2013) and can be measure using most wireless devices easily as the RSS collection is supposed by almost all wireless chips. RSS is a measurement of the power of the radio signal at the

received end. RSS-based approaches have been extensively studied and have achieved good performance to identify different activities; for instance object tracking and location (Wilson and Patwari, 2010a, 2010b; Xiang, Ji, & Zhang, 2018; Youssef, Mah, & Agrawala, 2007), driving behavior (Lv et al., 2017), crowd counting (Depatla & Mostofi, 2018), hand gesture recognition (Haseeb and Parasuraman, 1707), etc. However, as the RSS is coarse-grained and can be easily corrupted by multipath effect, these RSS systems often require a line-of-sight (LOS) transmission, resulting in a limited accuracy in indoor activity detection (Xu, Han, Wang, Wu, & Liu, 2019).

To improve the accuracy of WiFi sensing, CSI has become a good alternative. CSI contains more detailed information due to its high dimension structure, thus it can support fine-grained classification applications (Xu et al., 2019). CSI can be expressed as a complex matrix, where each entry represents the amplitude and the phase response of the signal transmission channel. Therefore, the amplitude of the CSI signal quantifies the signal power attenuation after the multi-path effect (similar to signal strength) (Xu et al., 2019). Multiple system has been developed on monitoring activities using variations and statistics of CSI; for example, small hands motions (Ali, Liu, Wang, & Shahzad, 2015; Tan & Yang, 2016), indoor human activities (Wang et al., 2014, 2017a; Wu et al., 2015; Zeng, Pathak, Xu, & Mohapatra, 2014), human behavior recognition (Wang et al., 2019), traffic monitoring (Won, Zhang, & Son, 2017), fire detection (Zhong et al., 2017), wheat moisture detection (Yang et al., 2018a), object distinction (Zou, Wang, Ye, Wu, & Ni, 2017), school violence monitoring (Zhou et al., 2017), etc.

Another category of wireless passive sensing techniques relies on the FMCW information embedded in the received signals to track changes of reflected objects for motion detection or vital sign monitoring (Xu et al., 2019). ToF (Banin, Schatzberg, & Amizur, 2013) is a time-based range measurement protocol that aims to provide high accuracy positioning information. Some of the applications using ToF includes vital sign detection (Adib et al., 2015a; Zhang, Hu, Chen, & Zeng, 2019), gain patterns (Adib et al., 2015b; Raj, Chen, & Lipps, 2010; Tahmoush & Silvious, 2009), location (Adib et al., 2014, 2015c), etc. The main problem is ToF-based wireless sensing systems rely either on large sensing bandwidths (Nanani & Kantipudi, ; Zhu, Zhu, Zhao, & Zheng, 2015) or specially designed frequency-modulated continuous-wave signals (FMCW) (Adib et al., 2014, 2015a). Therefore, those ToF cannot be implemented on off-the-shelf WiFi devices and their ability of detecting multiple indoor events has not been studied yet.

Here, we aim to present the currently available approaches to estimate vital signs, specifically RR (also known as breath rate) using different types of wireless sensing techniques, and propose a reliable framework for applying the best-fit technology for real-time monitoring of COVID-19 patients. Then, the following approaches are categorized into three groups: RRS-based, CSI-based, and ToF-FMCW based approaches for RR estimation. Fig. 1 shows an illustrative taxonomy of the investigations that have been done in this field.

2.1. RRS-based approaches for RR estimation

Initially, RRS-based methods were utilized to locate people inside buildings using static wireless networks to measure links RSS values (Kanso & Rabbat, 2009; Patwari & Agrawal, 2008; Woyach, Puccinelli, & Haenggi, 2006; Zhang, Ma, Chen, & Ni, 2007; Zhang & Ni, 2009). The location also can be done through walls (Maas, Wilson, & Patwari, 2013; Wilson & Patwari, 2010a, 2010b; Zhao & Patwari, 2011; Zheng & Men, 2012) using a variety of statistics of the measured RRS. Later multiple applications have been developed in the healthcare area. *Patwari* et al. (Patwari et al., 2014b) explored the use of RSS measurements on the links between wireless devices to identify where a breathing person is located and estimate RR in a home, while the person is sitting, lying down, standing, or sleeping. The main idea of RSS-based breathing location is based on the assumption that a link's RRS measurement is sensitive to the
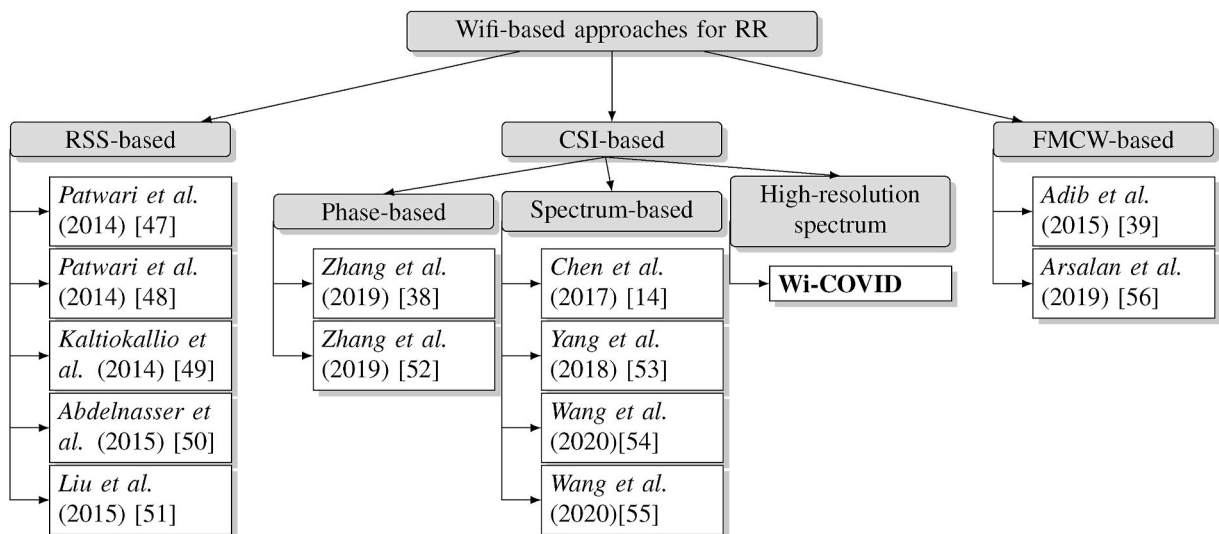

Fig. 1. WiFi-based approaches for RR extraction.

breathing movement when a person breaths near the link line, and there is no more motion around. Furthermore, authors of (Patwari et al., 2014b) addressed the challenge of detecting breathing when the person occasionally moves by using a change detector across the links. For RR estimation, they used a method presented in their previous work (Patwari et al., 2014a), which calculates the power spectral density (PSD) over each link using the most recent samples, sums the PSD over all links, and estimates RR as the frequency at the maximum of the sum PSD. The main challenge faced was that usually the link that better measures chest movement is the link that measures other movements (motion interference). Therefore, the authors proposed a combination of Welchs t-test (Kay, 1993) and Wilcoxon rank-sum test (Wilcoxon, 1992), which are change-point detection methods. Their proposed method was to use the detected break-point indices to remove the mean from the raw RSS and use the residual RSS for RR estimation. Even though the method allows small movements, the reliability of the RSS links with large noise makes the method unstable for measuring respiration.

More recently, some respiration monitoring systems based on commercial off-the-shelf transmitter-receiver were proposed. In (Patwari et al., 2014b), the RRS measurements of a network of transceivers are utilized for extracting RR, which was improved by (Kaltiokallio, Yiğitler, Jäntti, & Patwari, 2014) where RSS data from a single TX-RX pair can identify ones RR. The RSS, however, is not a sensitive indicator for reliably tracking minute chest movement. Exhaling and inhaling causes very small changes in RSS and these changes can be easily polluted by other factors and environmental noise. *Abdelnasser* et al. (Abdelnasser, Harras, & Youssef, 2015) proposed a full architecture for extracting breathing signals from noisy WiFi RSS. Various challenges were addressed like noise elimination, interfering with humans, sudden user movements, as well as detecting abnormal breathing situations. The framework claims the detection of apnea situations with more than 96% of accuracy. The framework includes a breathing signal extractor, which relies on frequency spectrum obtained by applying fast Fourier transformation (FFT) to a sliding window of the WiFi raw signal and a bandpass filter to limit the frequencies to those within the range of the normal human breathing (between 0.1 and 0.5 Hz) (Lindh, Pooler, Tamparo, Dahl, & Morris, 2013). RR ($\widehat{r}$) is finally estimated as the frequency with the maximum magnitude in the human RR range as shown in the equation:

$$\widehat{r} = \underset{r_{min} \leq r \leq r_{max}}{\operatorname{argmax}} |\text{FFT}(x_{1..n})| \tag{1}$$

where r_{min} is the minimum RR, r_{max} is the maximum RR, and $x_{1..n}$ are the RSS values in the current sliding window. Once the breathing is estimated, a RR extractor is applied by fusing different overlapping consecutive windows in order to obtain a stable consecutive reading. The authors in (Abdelnasser et al., 2015) also developed a method for detecting apnea using the extracted RR. To do so, they applied a discrete wavelet transform (DWT) and a thresholding method.

Even though RR was extracted with RSS-based WiFi information, because RSS is coarse-grained, it has multiple limitations. For instance, in the previous works, the accuracy can be diminished and corrupted by the multipath effect. In wireless sensors, due to reflections, multiple copies of the same signal arrive at the receiver, each undergoing different delays and attenuations. This effect is known as multipath (Sen, Lee, Kim, & Congdon, 2013). For this reason, the RSS-based sensing system often requires a line-of-sight (LOS) transmission, which means the person has to be closer to the LOS system, resulting in a limited accuracy in indoor activity detection. The RSS, however, has found to be insensitive for reliably tracking the minor chest movement due to respiration, as the RSS changes caused by exhaling and inhale are so small that they can be easily submerged by environmental noise (Liu, Cao, Tang, Wen, & Guo, 2015).

2.2. CSI-based approaches for RR estimation

While the RSS-based methods are found to be workable only when the subject stays close to the LOS, the CSI-based methods seem more appealing as they can capture the subjects RR from a distance, making it viable for long-term RR monitoring. In general, the CSI-based methods can be classified into three categories:

2.2.1. Phase-based CSI

Phase-based methods exploit the phase information of the signal. In 2019, Zhang et al. (Zhang et al., 2019) proposed a contact-free breath tracking system, BreathTrack. Authors used a Hampel filter, an FIR high pass filter (cut-off frequency is 0.05 Hz) in order to eliminate low-frequency noise and avoid phase distortion. Also, authors adopted an AoA-TOF sparse recovery method to obtain the phase variation of attenuation coefficient and acquire respiratory state and RR. *Zhang et al.,* (Zhang et al., Liu) presented the model, design, and implementation of a sleep monitoring system that exploits ambient radio signals to recognize sleep stages and assess sleep quality including RR by setting up one single link between two commodity radios. Authors adopted a statistical approach by examining the auto-correlation function (ACF) of CSI power response, which significantly shortens the time delay and produces the instantaneous estimation. Based on the calculated ACF, the approach first detects the presence/absence of breathing. Then, if present, it estimates RR by extracting following features: peak prominence, peak amplitude, motion interference ratio, and peak location. In general, the larger the motion statistic, peak prominence, peak width, peak amplitude and the smaller the motion interference ratio, the more likely is the presence of the breathing signal. Once there is a breathing signal, RR can be estimated as $RR = 60/\widehat{\tau}$, where $\widehat{\tau}$ is the location of the first dominant peak.

The phased-based CSI methods assume only one person in the observation area, as the spatial resolution of these systems is too low to distinguish the RF signals reflected by multiple users. In addition, note that (Zhang et al., 2019) argued that the method (Wang et al., 2017b) that utilizes the phase difference between antennas to eliminate phase distortions introduced in the internal circuit is inaccurate. Because the phase of measured CSI on all antennas are affected by the minor displacement caused by breath, phase difference

between antennas is actually the subtraction of two periodic signals instead of the real respiratory movements.

2.2.2. Spectrum-based CSI

It is the most common used method for extracting respiration with CSI-based WiFi approach. In 2017, *Chen* et al. (Chen et al., 2017) introduced TR-BREATH, a contact-free breathing monitoring system leveraging time-reversal (TR) technique that detects and monitors multi-person breathing utilizing the CSIs obtained from off-the-shelf WiFi devices. TR-BREATH could capture the minor but periodic variations in CSIs caused by breathing. Authors of (Schmidt, 1986) used Root-MUSIC algorithm to achieve highly accurate RR estimations within 10 s. The method consists on 1) calculating the time-reversal resonating strength (TRRS) (Wang, Wu, Han, Yang, & Liu, 2011); 2) analyzing the calculated TRRS with the Root-MUSIC (Rao & Hari, 1989) to produce RR candidates; 3) deriving key statistics based on these candidates to facilitate breathing detection; 4) estimating the multi-person RRs via affinity propagation (Frey & Dueck, 2007), likelihood assignment, and cluster merging; and 5) formulating an estimation on the number of people based on the cluster likelihoods.

Later, in 2018, *Yang* et al. (Yang et al., 2018b) applied the Hampel filter (Davies & Gather, 1993) and wavelet filter (Villasenor, Belzer, & Liao, 1995) on the CSI series to remove outliers and high-frequency noises. Then, RR is estimated by performing FFT on all the CSI streams targeting frequencies between 0.1 Hz and 0.6 Hz. They applied the technique to study the problem of multi-person sleeping respiration monitoring using CSI-based method and COTS WiFi devices. They employed one transmitting (Tx) and two receiving antennas (Rx1 and Rx2), forming two pairs of transceiver antennas (Tx-Rx1 and Tx-Rx2). Each transceiver antennas pair creates a series of concentric Fresnel zones. However, two or more persons in the room have to breathe in different rates and be near to the Fresnel zones to be detected.

Wang, Zhang, Wu, Wang, & Liu, (Wang et al., Lu) proposed a continuous RR tracking system of multiple persons using the CSI of a single pair of commercial WiFi devices. The authors eliminated assumptions like a fixed number of people in the area of interest. Authors proposed three steps: 1) multi-user breathing spectrum generation; 2) RR trace tracking; and 3) people counting and recognition. For RR extraction, they first applied a short-term Fourier transform (STFT) on CSI measurements to extract periodic breathing signals. If multiple people in the room, different frequency responses will be observed as people breathe at different rates. They applied an adaptive sub-carrier combining method to make the signals stronger and provide a spectrogram of the estimated RRs over time. Lately, in 2020, *Wang et al.* (Wang, Zhang, Wu, Wang, & Liu, 2020) also present a calibration-free remote vital sign monitoring system that can simultaneously monitor multiple users by leveraging CSI of 60 GHz WiFi. They applied a spectrum analysis as the breathing signal is periodical. To utilize a correct window size at the signal for frequency resolution, the authors adopted a statistical approach by examining the ACF of the candidate CSI phase. Purely spectrum-based CSI methods require a large delay (e.g., more than 30 s) to gain better frequency resolution, and cannot observe immediate RR changes, since RR is assumed to be constant within the time window.

2.2.3. High-resolution spectrogram based CSI

For effective RR estimation, we propose a high-resolution spectrogram based CSI approach for the Wi-COVID framework. The proposed approach combines advanced signal pre-processing techniques to effectively extract the target signal component, and the high resolution spectrogram to obtain an accurate and dynamic RR estimation. The proposed flowchart is displayed in Fig. 2, and more details are discussed in this subsection. The CSI signal processing consists of the following steps: (1) Obtaining CSI signal magnitude; (2) Removing outliers by the Hampel identifier (Liu, Cao, Tang, Wen, & Wi-sleep, 2014), and using a bandpass filter with cut-off frequencies of 0.2 Hz and 0.4 Hz to suppress the noises; (3) Using principal component analysis (PCA) to extract respiration component, and then applying high resolution spectrogram to extract the instantaneous frequency of the respiration component to estimate RR; (4) Calculating the shortness of breath indicators in both time and frequency domains to evaluate the COVID-10 symptoms.

The first step of CSI processing is to remove the noise interference. There could be abnormally sudden changes in the collected CSI data due to equipment and environment. We propose to use the Hampel filter to suppress the strong abnormal amplitudes, following Wi-Sleep (Liu et al., 2014) and WiHACS (Chowdhury, Leung, & Miao, 2017). The noise, especially amplitude outliers, will be wiped out and replaced by the moving average of their neighboring data samples. Besides, the Hampel filter could also remove the impacts of invalid CSI data samples caused by the sensing or data transmission. Note that if after the Hampel filter, there are still noises left, a classic moving average filter can be applied to smooth the data (Dixon and Massey). After removing the outliers, a bandpass filter is applied, which is an ordinary method that only allows signal components between certain frequency bands to pass. Since human
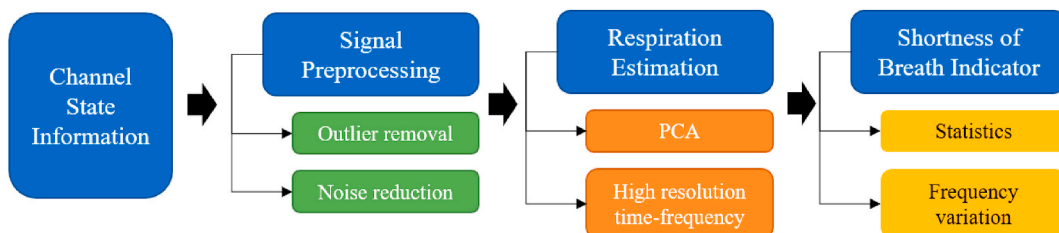

Fig. 2. Wi-COVID algorithm flowchart of the CSI based RR estimation and shortness of breath for COVID patient monitoring.

respiration activities fall into a specific frequency band of the CSI signals, the bandpass filter can effectively wipe out low-frequency and high-frequency noise interferences (Tataraidze, Olesyuk, & Pikhletsky, 2019). Note that in our study, we set up the analysis frequency band between 0.2 Hz and 0.4 Hz, which is a typical frequency range for human respiration (Clemente et al., 2020; Li et al., 2018a).

As indicated in A, CSI data have multiple channels from different sub-carriers. The respiration movements are hidden in the high dimensional data matrix. In order to extract the respiration related signal component, we propose to use the PCA technique (Gao, Lu, Li, & Jiang, 2013; Wold, Esbensen, & Geladi, 1987), which is a latent space projection method. The principle component calculated by PCA can represent the primary data features. Besides the data dimensionality reduction, the utilization of PCA can also enhance the data processing efficiency. In addition, in CSI-based human activity analysis, PCA can also be used for noise suppression and data redundancy reduction, e.g., Wi-Wri (Cao, Chen, & Zhao, 2016), WiHACS (Chowdhury et al., 2017), etc. Here, we use PCA to extract the principal respiration features, but in the meantime, various noises are removed as a side benefit.

Before introducing the high-resolution spectrogram, we first define the respiration related signal expression. The target non-stationary biomedical signal $f(t)$ can be defined as a summation of K oscillatory modes (Li et al., 2018b, 2019):

$$f(t) = \sum_{k=1}^{K} \alpha_k(t) s_k(2\pi N_k \varphi_k(t)) + \sigma(t) r(t), \tag{2}$$

where, $\alpha_k(t)$ is the instantaneous amplitude (IA), $N_k \varphi_k(t)$ is the instantaneous phase (IP) whose derivative is the instantaneous frequency (IF), $\{s_k(t)\}_{1 \leq k \leq K}$ are 2π-periodic and zero-mean wave-shape functions with a unit norm in $L^2([0, 2\pi])$, σ is a slowly varying smooth function and $r(t)$ is a random residual describing the noise. Note that the respiration component can be viewed as one oscillatory mode of the obtained CSI data. More specifically, in the pre-processed results, the respiration mode can be the primary mode.

To estimate RR, i.e. the IF of the respiration component, a time-frequency (TF) representation, e.g. STFT (Korany, Karanam, Cai, & Mostofi, 2019), can be utilized. As a classic TF representation, STFT expression can be given as:

$$V_f^{(h)}(t, \xi) = \int f(\tau) h(\tau - t) e^{-i2\pi\xi(\tau - t)} d\tau, \tag{3}$$

where, h is the window function, t indicates time, and ξ indicates frequency. This equation means that a short moving window is applied to the target signal f and the Fourier Transform is applied to each instance of the moving window to estimate the frequency components, resulting in a TF domain spectrogram.

Although as a classic TF method STFT has been widely applied, STFT has a relatively low TF resolution because of the uncertainty law (Lu & Li, 2013; Liu et al., 2017, 2020). However, for the dynamic RR estimation, we need to have a superior TF resolution to obtain an accurate estimate. To improve the TF resolution, a lot of efforts have been carried out, such as the wavelet synchrosqueezed transform (WSST) (Yang, 2015). In Section 5.2, we use real CSI data to demonstrate the TF resolution difference between STFT and WSST. The WSST which is a frequency reassignment method based on STFT ($V_f^{(h)}(t, \xi)$) can be defined as (Yang, 2015):

$$SV_f^{(h,v)}(t, \xi) = \int V_f^{(h)}(t, \eta) \frac{1}{\alpha} g\left(\frac{\left|\xi - \Omega_f^{(h,v)}(t, \eta)\right|}{\alpha}\right) d\eta, \tag{4}$$

where $\Omega(\cdot)$ denotes the frequency reassignment vector.

In principle, the respiration component is more periodic in the rest mode than other interference. Thus, the target respiration component will form an energy ridge in the given spectrogram along the time with the slightly various frequency. Therefore, we propose to extract the traces of successive RR component, which concatenates over both time and frequency in the given TF domain. For a given WSST spectrogram SV defined in Eq. (4), a reasonable estimate of the respiration component can be obtained by

$$\mathbf{g}^* = \underset{\mathbf{g}}{\operatorname{argmax}} E(\mathbf{g}), \tag{5}$$

where $\mathbf{g}$ indicates the respiration component, denoted as $\mathbf{g} := (g(n), n)_{n=1}^{I}$ is a mapping indicating the frequency component of the trace at the given time. $E(\mathbf{g})$ is the power of the processed CSI data, defined as

$$E(\mathbf{g}) = \sum_{i=1}^{I} SV(i, g(i)), \tag{6}$$

where $SV(i, j)$ denotes the WSST spectrogram at time bin i and frequency component j.

Assuming RR does not fluctuate a lot over a short period, a regularization term, e.g. a cross-entropy based criterion, can be applied to penalize sudden changes in frequencies of interests, in order to improve the temporal smoothness. Then, the optimal respiration component (energy ridge) can be extracted by solving the following problem:

$$\mathbf{g}^* = \underset{\mathbf{g}}{\operatorname{argmax}} E(\mathbf{g}) - \lambda C(\mathbf{g}), \tag{7}$$

where λ is a regularization factor of the penalized energy $C(\mathbf{g})$ (Wang et al., Liu).

Finally, we define the shortness of breath indicators in the time domain I_1 and frequency domain I_2. The time domain indicator characterizes the extracted respiration component local minimums and maximums following:

$$I_1 = \frac{\sum_{i,j\in\mathfrak{W},i\neq j}|\max_i - \max_j| + \sum_{i,j\in\mathfrak{W},i\neq j}|\min_i - \min_j|}{\Omega}, \tag{8}$$

where, max and min represent the local extrema, i.e., peaks and troughs of the respiration oscillation. $\mathfrak{W}$ denotes the analysis window, and Ω is a factor to balance the amplitude variation. If there is no obvious amplitude change, I_1 will be relatively small to indicate a smooth respiration, while sudden amplitude changes will significantly change I_1.

The frequency indicator leverages the gray level co-occurrence matrix (GLCM) (Qi, Lin, Zhao, Li, & Marfurt, 2016; Zou, Wang, Li, & Song, 2018) of the spectrogram. The GLCM entropy characterizes the complexity of the image texture, so we use it to analyze the spectral variations as:

$$I_2 = -\sum_{i=0}^{n-1}\sum_{j=0}^{n-1} p(i,j)\log_b p(i,j), \tag{9}$$

where n and b are the number of gray levels and the base of the logarithm function, respectively. $p(i,j)$ stands for the probability of two pixels separated by the specified offset having intensities i and j. If there is no obvious frequency variation, I_2 will be relatively small because the spectrogram has a low complexity, vice versa.

2.3. FMCW-based approaches for RR estimation

The frequency modulated continuous wave (FMCW) has been first used to detect human respiration using acoustic signals by measuring the chest movement displacement during breathing (Nandakumar, Gollakota, & Watson, 2015). *Adib* et al. (Adib et al., 2015a) introduced Vital-Radio, a wireless sensing technology that monitors breathing and heart rate. The approach exploits the fact that wireless signals are affected by motion in the environment, including chest movements due to inhaling and exhaling and skin vibrations due to heartbeats. Specifically, it transmits a low-power wireless signal and measures the time it takes for the signal to reflect back to the device. The reflection time depends on the distance of the reflector to the device, and changes as the reflector move. Based on this idea, the approach uses a radar technique called FMCW to separate the reflections arriving from objects into different buckets depending on the distances between these objects and the device. In theory, the procedure in (Adib et al., 2015a) consists on 1) isolate reflection from different users and eliminate reflections that come from furniture or walls using FMCW as a filter; 2) identifying reflections involving RR and heart rate by determining different travel distances from the device and measuring the resulting variations in the phase of the reflected signal. If period variations are obtained, they assume respiration or heart, depending on the frequency; and 3) extracting the RR and heart rate by performing an FFT. The peak at the output of the FFT will correspond to the dominant frequency, which they assume to be the RR. However, the above approach requires specialized and expensive hardware and cannot give precise estimation if the two persons are too close to each other.

Later, *Arsalan* et al. (Arsalan, Santra, & Will, 2020) tried to improve the RR and heartbeat estimation with FMCW Radar. To enhance the stability and accuracy of the detected RR and heart rate, the authors used a Kalman filter-based tracking of the heartbeat signal. After providing an initial rough estimation, the applied bandpass filter bandwidth is successively narrowed down, and the filter limits are steadily updated to the current heart rate of the target. Measurement segments with random body movements are automatically identified and consequentially ignored for the Kalman filter update. However, the approach was not directly applied to signals coming from WiFi and complicated apparatus to be used.

In general, FMCW-based WiFi approaches require specially design transmission signals, high sounding rate and large antenna arrays, huge transmission bandwidth (over 1.7 GHz), cannot be integrated with a commercial WiFi, and device calibration and specially design hardware required (Xu et al., 2019). For those reasons, the FMCW-based approach is not suitable for long-term monitoring and its complicated setup is infeasible for patient supervision.

3. Framework Overview

COVID-19 has raised huge challenges to the healthcare system around the world. Countries like China, Italy, and the United States have witnessed that the pandemic overwhelms their hospitals and posts a critical problem to assist thousands of patients at the same time. To reduce the burden on health-care systems, patients with COVID-19 are triaged based on the severity of the disease, so mild and asymptomatic cases are treated at home unless rapid deterioration occurs (Home care for patients wi). Being able to monitor real-time RR remotely using noninvasive sensing can provide more accurate alerts of sudden changes and potentially identify patient deterioration. In this section, we present an overview of the WiFi-based real-time sensing along with tele-health using a Cloud, called Wi-COVID, that can monitor symptoms and warning signs in COVID-19 patients. Wi-COVID will potentially reduce face-to-face contacts and enable better management via early detection. If RR deteriorates, the data sent via a secure Cloud platform can enable healthcare practitioners to perform effective general population triage such as placing patients under self-isolation, transferring patients to hospitals, managing high-risk population even if they do not present symptoms, etc.

Wi-COVID framework consists of three layers as shown in Fig. 3. The layers provide abstraction in the recognition process as we can

separate the signals from the WiFi devices in the "sensing layer" using a commercial device like Raspberry PI, process and estimate RR from the CSI signals using the proposed method introduced in Section 2.2.3 in the "processing layer" using the Cloud, and provide real-time visualization and alerts using a stream database and powerful visualization (like Grafana tool (Clemente et al., 2020)) in the "monitor layer".

3.1. Sensing layer

The sensing layer of Wi-COVID framework is composed by a off-the-shelf WiFi device and a Raspberry Pi that acts like a WiFi Access Point (AP). As it is going to be explained in Section 4.1, we utilize BCM43455C0 WiFi chip used in Raspberry Pi 4 for extracting CSI of OFDM-modulated Wi-Fi frames (802.11n) on a per frame basis with up to 80 MHz bandwidth. In Fig. 3, this is called WiFi AP. In general, the WiFi AP signals can be collected using certain API software (Gringoli et al., 2019), such as Nexmon (Schulz, Wegemer, & Hollick, 2017).

For the RR extraction of COVID-19 patients, the person has to be in the cover area of the WiFi and in a resting mode (either sleeping on a bed, or setting, or standing without walking). The phase of the data batches is accurate enough to discern the small body movements caused by respiration. If the person is located in the next room with a wall in the middle, we are still able to get the RF signals, and some filters, like Hampel filter (Davies & Gather, 1993), are needed to remove outliers and superfluous information. The information is gathered using a Raspberry Pi 4 on each scenario, which guarantees a cheap way to process WiFi information. Once the information from the CSI is extracted, the device is ready to process the RR extraction. Note that all the methods to extract respiration are done in-situ, which means that the processing is made inside the Raspberry Pi.

3.2. Processing layer

Once the CSI information has been extracted, the device perform the proposed method explained in Section 2.2.3 to estimate RR. RR is extracted continuously from the information come from CSI and the results are sent to a Cloud for visualization. We use InfluxDB (Naqvi et al. Zimányi) database to save the information. The transmission process is done in secure way by utilizing HTTPS API of InfluxDB. The idea of using InfluxDB allows to store stream data in a simple way and can be visualized with standard tools like Grafana (Beermann et al., 2020). In this type of setup, the framework allows to collect data from different rooms or houses to the same database, and it allows to visualize multiple users at the same time, which extend the functionality of the system.
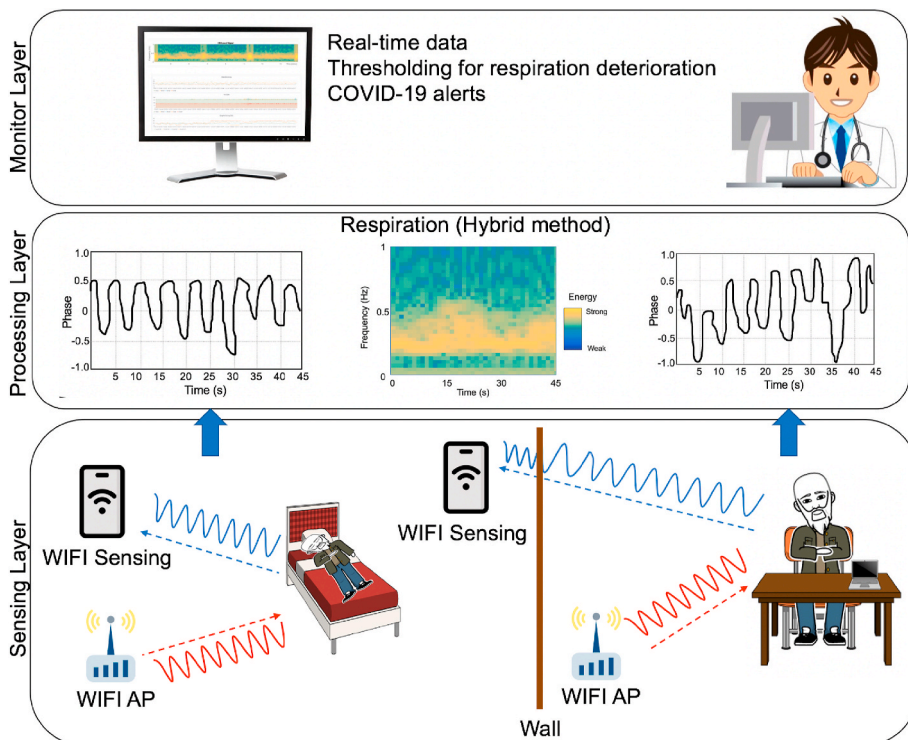

Fig. 3. Wi-COVID framework overview.

3.3. Monitor layer

Because results of the patient RR are stored in the Cloud, the healthcare provider can access patient's information in real-time. Furthermore, we have utilized the Grafana visualization to allow the provider to set up alarms when the RR passes certain thresholds. When Grafana detects an "unusual" respiration value, it triggers an alarm in the dashboard which allows the healthcare provider to visualize the current status of the patient. Moreover, the practitioner can visualize the past data by selecting the date range. Then, the framework allows to visualize both current RR and historical information, which helps the decision making process. Fig. 4 demonstrates the monitor layer showing three different patient's RRs obtained by Wi-COVID.

4. Prototype system

In this section, we explain the hardware and software used for the Wi-COVID implementation. In order to make Wi-COVID economically attractive, instead of complicated devices or the use of laptops to capture the signals, we propose the use of a simple Raspberry Pi that will act as an kind of access point. In the software side, we use open-source codes for implementing the CSI processing in the Raspberry Pi.

4.1. Hardware

Nexmon firmware patching framework (Schulz et al., 2017) was proposed to enable researchers access to lower-layer frame processing and advanced physical-layer functionalities on Broadcom WiFi chips. It allows users to create firmware modifications for embedded ARM processors using C code. Currently, the framework supports Raspberry Pi implementations. We used Nexmon to extract CSI of OFDM-modulated WiFi frame 802.11n on a per frame basis with up to 80 MHz bandwidth on the Broadcom WiFi chip of the Raspberry Pi. Then, our implementation is simpler than others as we only need a off-the-shelf WiFi router and a Raspberry Pi.

4.2. Software specification

Multiple software and packages were used to develop Wi-COVID framework. In this section we mention the different integrated software applications used for the proposed framework.

4.2.1. Software to extract CSI
As mentioned, we use the Nexmon framework to read CSI. Each User Datagram Protocol (UDP) packet containing collected CSI has 10.10.10.10 as the source address and is destined to 255.255.255.255 on port 5500. The payload starts with four magic bytes 0×11111111, followed by the six byte source mac address as well as the two byte sequence number of the WiFi frame that triggered the collection of the CSI contained in this packet. The next two bytes contain core and spatial stream number where the lowest three bits indicate the core and the next three bits the spatial stream number, e.g. 0×0019 (0b00011001) means core 0 and spatial stream 3. The chanspec used during extraction can be found in the subsequent two bytes. After two bytes identifying the chip version, the actual CSI data follow.

4.2.2. Software to estimate RR
Inside the device (Raspberry Pi), we use the Python code to analyze the Wi-COVID data and estimate RR. The extracted respiration
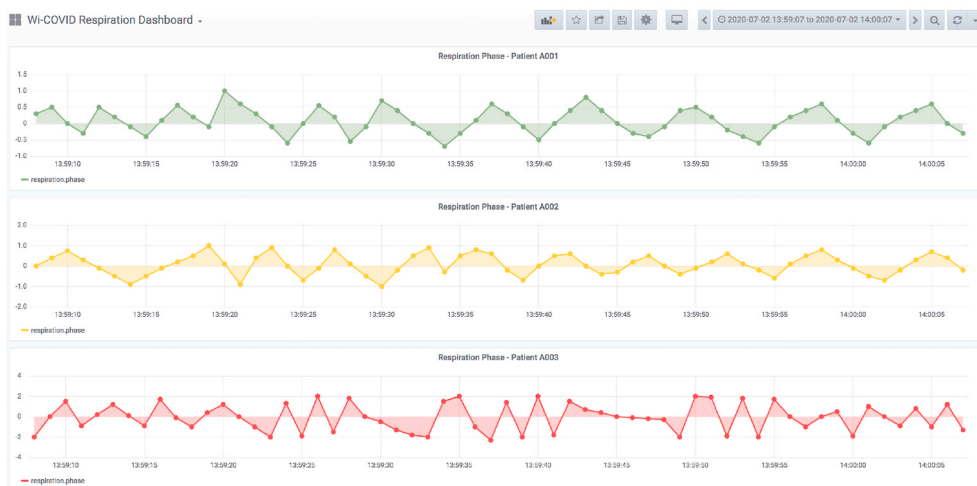

Fig. 4. Monitor layer for RR obtained by Wi-COVID.

is send to a Cloud database using a HTTPS service. The used database is InfluxDB (Naqvi et al. Zimányi). InfluxDB is an open-source time series database developed by InfluxData (InfluxOpen Source Time). It is written in GO and optimized for fast, high-availability storage and retrieval of time series data in fields such as operations monitoring, application metrics, Internet of Things (IoT) sensor data, and real-time analytics.

4.2.3. Software to monitor and alert patient's condition

Once the RR information is stored in InfluDB, we use Grafana (Beermann et al., 2020) for visualization. Grafana is a multi-platform open source analytics and interactive visualization web application. It provides charts, graphs, and alerts for the web when connected to supported data sources. It is expandable through a plug-in system. End users can create complex monitoring dashboards using interactive query builders. We configure alerts inside Grafana to notify users in real-time when RR is abnormal. The anomaly in this case is defined as bypassing the lower threshold or the upper threshold that would trigger an alert when the counting on the respiration (RR) measurements. The alert helps the healthcare provider to visualize the real-time and historical data of the specific patient.

5. Evaluation

In this section, we present the preliminary results of the Wi-COVID implementation using a WiFi sensing and a Raspberry Pi, which provides an easy installation and a cheap alternative for COVID-19 patients and healthcare practitioners.

5.1. Experiment setup

COVID-19 patients with few, mild or no symptoms are typically instructed to perform self-quarantine at home. According to the CDC self-quarantine protocol (C and Coronavirus Disease, 2020b), if the COVID-19 diagnosed person is living with other people in the same house, this person needs to be isolated in a separate room. Following this guidance, we setup our experiment in a room with a WiFi sensing and Raspberry Pi as shown in Fig. 5.

CSI describes how an RF signal propagate from the TX(s) to the RX(s) and reveals the combined effect of, for instance, scattering, fading, and power decay with distance. With commodity WiFi Network Interface Cards (NICs), a group of 30 sub-carriers measurements can be revealed to upper layer users in the format of CSI. Each CSI depicts the amplitude and phase of a sub-carrier. Fig. 6 shows the amplitudes of CFR from three antennas, between 15 s and 30 s. From the CFR amplitudes of Antenna 1, we can clearly see some ripple-like pattern, which we will shown soon corresponds to the movement of chest. Likewise, the breath caused signal ripples can also be observed in the CFR amplitudes of Antennas 2 & 3. In the next subsection, we process the CSI data using the proposed method in Section 2.2.3 to get the RR estimate.

5.2. Preliminary results

Based on the findings shown in Fig. 6, the CFR amplitudes of CSI data are taken as the input for monitoring RR. In this section, we describe how the CSI data are processed for tracking RR step by step.

The first step is to remove outliers. In the collected CSI data, there are some abrupt changes of CFR amplitudes that are obviously not caused by the movement of human chests, but the noise interference. Fig. 7a shows the CFR from all the 30 sub-carriers of Antenna 3 from Fig. 6. It can be seen that there are some significant abrupt change points of the CFR in some or all sub-carriers, e.g. 21 s, 25 s and 30 s, which are outliers and must be eliminated. We utilize the Hampel identifier (Liu et al., 2014) on all the 30 sub-carriers. Fig. 7b
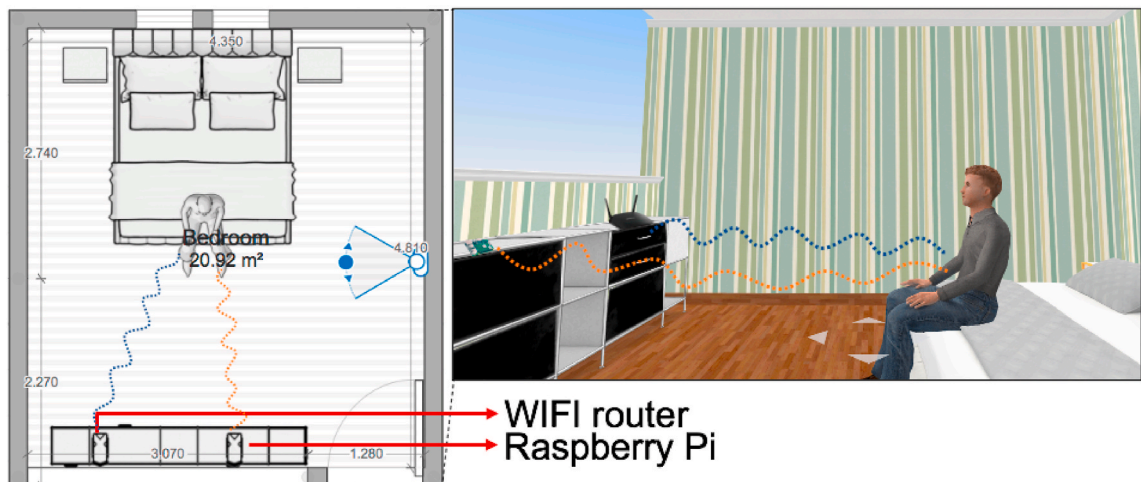

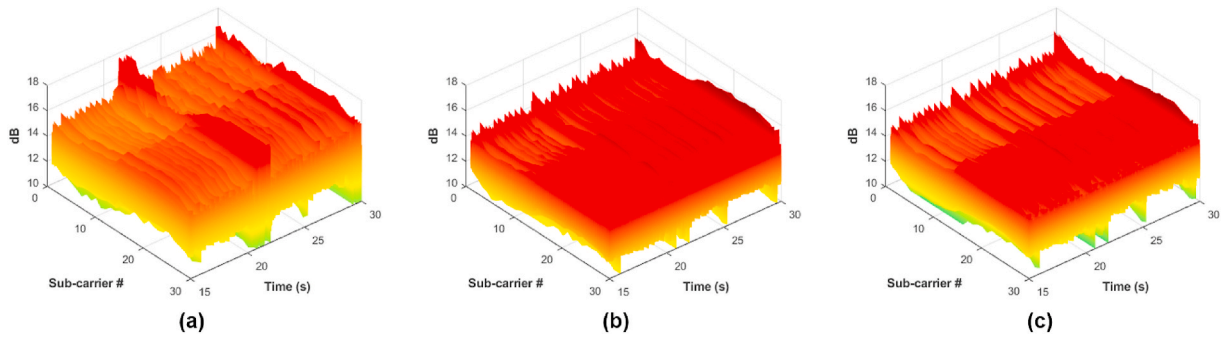**Fig. 5.** Wi-COVID experiment setup for COVID-19 self-quarantine patients.

Fig. 6. The channel frequency response (CFR) amplitudes from Antennas (a) 1, (b) 2, and (c) 3.
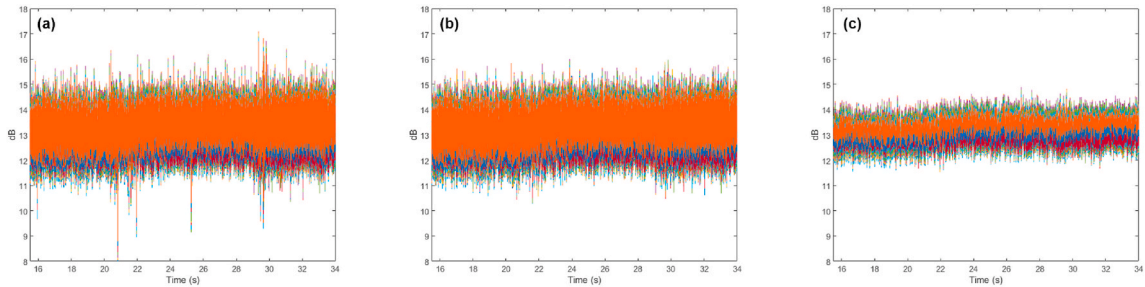

Fig. 7. (a) The original CFR from all 30 sub-carriers of an antenna. (b) The CFR after the outlier removal using the Hampel filter. (c) After moving average filtering.

shows the results after all the identified outliers have been removed, indicating that the Hampel identifier performs very well. In order to further smooth the CSI data, we apply a moving average filtering and obtain the filtered results shown in Fig. 7c, where the noise has been significantly reduced.

After the outlier removal and noise reduction, we apply the bandpass filter to extract the respiration component, as shown in Fig. 8. Now we can observe the respiration oscillations very clearly. However, because of the different spatial placements of the antenna arrays, each channel represents different CSI information propagated from different paths. This is the reason that though they are representing the same information, the CSI channels do not fully overlap on each other in Fig. 8. Therefore, we apply PCA to extract the principal signal component. Fig. 9 shows the extracted respiration component, where we can observe the chest movement pattern clearly.

To obtain the IF of respiration component, we calculate the STFT and WSST spectrograms, which are shown in Figs. 10 and 11, respectively. It is clear that the WSST representation has a superior TF resolution, which is beneficial for an accurate IF estimation. Using the energy ridge extraction method defined in Eq. (7), we can obtain the dynamic IF of respiration component. Then $RR = IF \times 60$ bpm. Need to mention, alternatively, applying the FFT to the extracted respiration component can also generate the spectrum as shown in Fig. 13. However, it is clear that the FFT spectrum has a low resolution and carries much less information than the spectrogram, especially the temporally instantaneous information (Fig. 12).

To evaluate the shortness of breath indicators, we demonstrate another example in Fig. 14. The participant pretends to have a shortness of breath between 20 s and 22 s. Then, the corresponding bandpass filtering results, respiration component extraction result, and the WSST spectrogram are shown in Fig. 15. Comparing Figs. 9 and 15b, we can observe that when there is a shortness of breath,
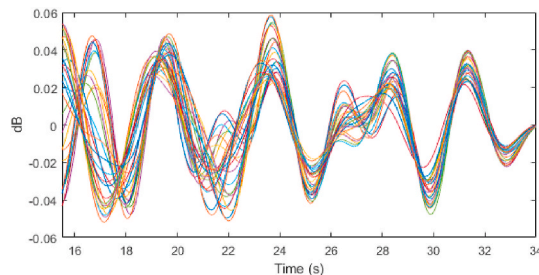

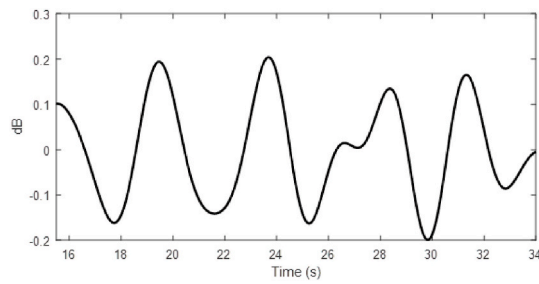**Fig. 8.** 30 CFR sequences after using the bandpass filter.

Fig. 9. The extracted principal signal component using PCA.
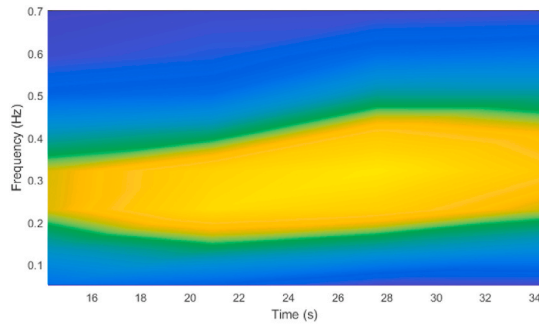

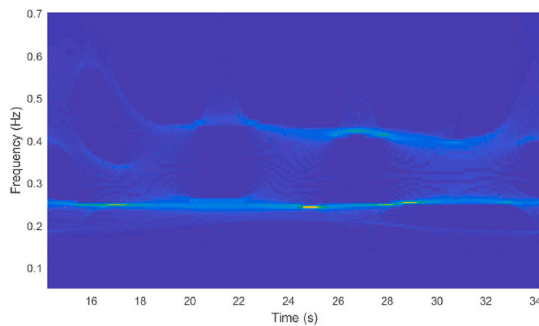**Fig. 10.** Time-frequency distribution using STFT.

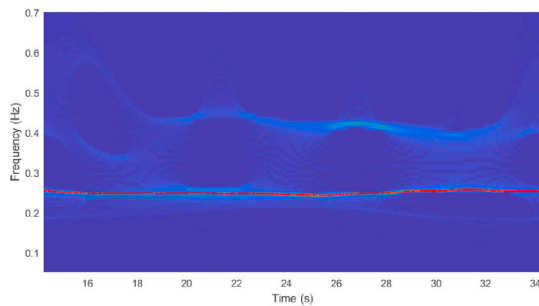**Fig. 11.** Time-frequency distribution using WSST.

Fig. 12. Instantaneous frequency extraction from WSST.

the amplitudes generate noticeable variations. $I_1 = 2.75$ for Fig. 9, while $I_1 = 7.2$ for Fig. 15b. Next, comparing Figs. 11 and 15c, it is clear that the spectral energy concentrates more in the first example. Quantitatively speaking, $I_2 = 0.453$ for Fig. 11, while $I_2 = 2.504$ for Fig. 15b. As we defined in Section 2.2.3, the smaller of the shortness of breath indicators, the smoother of the respiration. Thus, the
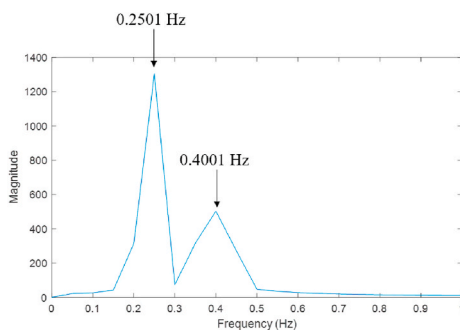
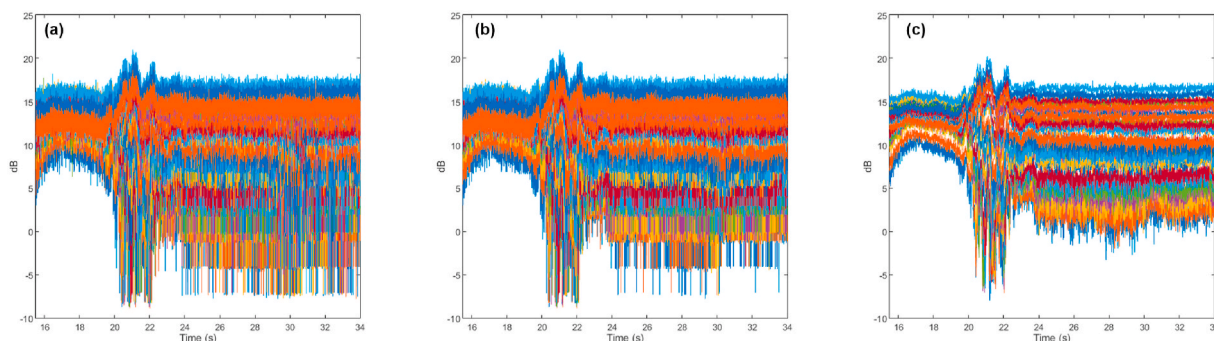**Fig. 13.** Peak frequencies estimated from FFT spectrum.

Fig. 14. Another example of the CSI processing following the same sequence of Fig. 7.
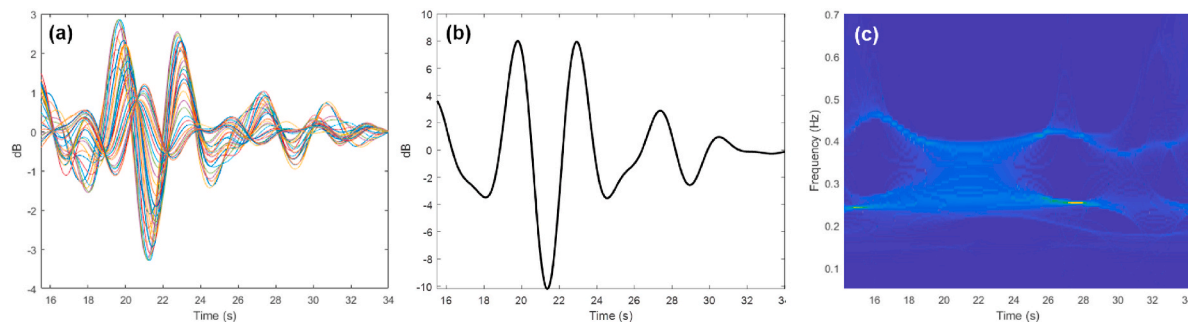

Fig. 15. (a) bandpass filtering results, (b) respiration component extraction result, and (c) WSST spectrogram calculated from the CSI data shown in Fig. 14.

preliminary results validate our proposed approach. Please notice that these are just preliminary results, and the criteria will be adjusted in the future to better differentiate normal breath and shortness of breath based on a larger dataset with more training data. Note that we adopt signal processing metrics to describe the breath shortness instead of the machine learning or deep learning models

Table 1
Comparison of features between Wi-COVID and other approaches.

Feature Proposed Work	CSI extraction	Respiration estimation	Shortness breath alert	In-situ Computing	Devices for AP
Wi-COVID	**Yes**	**Yes**	**Yes**	**Yes**	**Raspberry PI**
Chen et al. (Chen et al., 2017)	Yes	Yes	No	Yes	Cards in laptops
Zhang et al., (Zhang et al., Liu)	Yes	Yes	No	Yes	Special WiFi routers
Wang et al. (Wang et al., 2020)	Yes	Yes	No	No	Qualcomm 60 GHz chipset
Wang et al., (Wang et al., Liu)	Yes	Yes	No	Yes	Laptops
Zhang et al. (Zhang et al., 2019)	Yes	Yes	No	No	Antennas
Yang et al. (Yang et al., 2018b)	Yes	Yes	No	Yes	Laptop

because of the lack of training data and labels. In the future, more advanced methods can be developed with more avaible data.

5.3. Our advantages

Compared with other current approaches, Wi-COVID is the only one that uses simple and inexpensive devices to estimate RR from WiFi signals. Currently, Wi-COVID is the only solution that can alert shortness of breath to help to alert healthcare providers. In Table 1, we present the desirable features of a framework for monitoring COVID-19 patients in self-quarantine. The characterized features include:

- CSI extraction: Using WiFi signals and extracting CSI information are desirable. And it is possible to use off-the-shelf devices for monitoring respiration (breathing).
- RR estimation: The approach necessarily needs to measure respiration in order to determine the patient's condition.
- Shortness breath alert: The approach needs to generate an alert when alteration on breath occurs during monitoring. These alterations may indicate patient deterioration.
- In-situ computing: To make the approach light and save bandwidth during computation, it is required to perform the heavy tasks directly in the pervasive device, for example, the CSI feature extraction and the RR estimation.
- Device for AP: The type of device used should be accessible and inexpensive for the final user, in this case, the COVID-19 patient.

6. Future directions

There are several possible improvements in our system can be made in the future. So far, we have proved that our framework is able to successfully extract RR for COVID-19 analysis. The potential of Wi-COVID for monitoring RR on COVID-19 patients is broad. Our next step is to deploy the framework inside COVID-19 patients' houses to transmit the information directly to the healthcare provider. Also, we are going to work directly with doctors and nurses to identify potential respiratory warnings that can be an indicator of patient deterioration. Also, we plan to incorporate a contactless alert system, which sends emails, text messages, and even GOOGLE HOME or AMAZON ALEXA messages when the shortness of breath symptom appears.

7. Conclusion

In this paper, we present Wi-COVID, a framework to monitor respiratory rates (RR) of COVID-19 patients using a non-invasive, real-time, and at-home technology. The proposed framework uses the available WiFi signal generated by common-used equipment at home to monitor COVID-19 patients. Using the at-home WiFi signals, we propose a non-invasive and non-wearable technology to monitor the patient and communicate RR to the healthcare provider in real-time. We have presented a comprehensive review of the current methods for extracting RR using WiFi signals. Then, we present a new methodology for extracting RRs from CSI using *high-resolution spectrogram* method. In our methodology, we apply a signal pre-processing of the CSI using an outlier removal and a noise reduction method. Then, the RR estimation is made by applying PCA and a high-resolution time-frequency spectrogram method. Finally, the shortness of breath is estimated with statistics and frequency variation methods. All the estimations are done using a Raspberry Pi board with WiFi capabilities. The results are transmitted in real-time to a Cloud server where we configure a visualization tool that allows the medical practitioner to monitor the patient in real-time and verify current and historical respiration values. We have demonstrated that our current setup can extract the RR under self-quarantine and self-isolation circumstances.

A. CSI Basics

CSI is a metric that describes the channel properties of wireless communication links and the quality of the wireless channel. In the frequency domain, the CSI matrix can be defined as:

$$Y = H \times X + N, \tag{A.1}$$

where H is the channel matrix; the received and transmitted signal vectors are Y and X, respectively; N refers to an additive white Gaussian noise.

During respiration, the chest movement can induce Δd displacement of the human body, which can vary from 2 mm to 14 mm (De Groote, Wantier, Chéron, Estenne, & Paiva, 1997; Shafiq & Veluvolu, 2014). While breathing, apart from the signals of dynamic paths reflected by the human body, there are also static paths of signals, including the direct signals and those reflected by the stationary objects. Thus, the overall received signals is a combination of the direct and reflected signals. Denote $H(f,t)$ as the CSI measurement for the sub-carrier with carrier frequency f at time t. For the indoor environment with static and moving objects, $H(f,t)$ can be expressed as:

$$H(f,t) = H_s(f,t) + H_d(f,t), \tag{A.2}$$

where the static vector $H_s(f,t)$ involves the signals of static paths, and the dynamic vector $H_d(f,t)$ contains the reflected signals of the moving object. The amplitude of $H(f,t)$ can be derived as (Wang et al., 2016):

$$\left| H(f,t,\theta) \right|^2 = \left| H_s(f,t) \right|^2 + \left| H_d(f,t) \right|^2 + 2 \left| H_s(f,t) \right| \left| H_d(f,t) \right| \cos\theta, \tag{A.3}$$

where θ is the phase difference between the vector $H_s(f,t)$ and $H_d(f,t)$.

References

Abdelnasser, H., Harras, K. A., & Youssef, M. (2015). Ubibreathe: A ubiquitous non-invasive wifi-based breathing estimator. In *Proceedings of the 16th ACM international symposium on mobile ad hoc networking and computing* (pp. 277–286).

Adami, A. M., Hayes, T. L., Pavel, M., & Singer, C. M. (2006). Detection and classification of movements in bed using load cells. In *2005 IEEE engineering in medicine and biology 27th annual conference* (pp. 589–592). IEEE.

Adib, F., Hsu, C.-Y., Mao, H., Katabi, D., & Durand, F. (2015b). Capturing the human figure through a wall. *ACM Transactions on Graphics, 34*(6), 1–13.

Adib, F., Kabelac, Z., & Katabi, D. (2015c). Multi-person localization via {RF} body reflections. In *12th {USENIX} symposium on networked systems design and implementation ({NSDI} 15)* (pp. 279–292).

Adib, F., Kabelac, Z., Katabi, D., & Miller, R. C. (2014). 3d tracking via body radio reflections. In *11th {USENIX} symposium on networked systems design and implementation ({NSDI} 14)* (pp. 317–329).

Adib, F., Mao, H., Kabelac, Z., Katabi, D., & Miller, R. C. (2015a). Smart homes that monitor breathing and heart rate. In *Proceedings of the 33rd annual ACM conference on human factors in computing systems* (pp. 837–846).

Alaziz, M., Jia, Z., Liu, J., Howard, R., Chen, Y., & Zhang, Y. (2016). Motion scale: A body motion monitoring system using bed-mounted wireless load cells. In *2016 IEEE first international conference on connected health: Applications, systems and engineering technologies (CHASE)* (pp. 183–192). IEEE.

Ali, K., Liu, A. X., Wang, W., & Shahzad, M. (2015). Keystroke recognition using wifi signals. In *Proceedings of the 21st annual international conference on mobile computing and networking* (pp. 90–102).

Arsalan, M., Santra, A., & Will, C. (2020). Improved contactless heartbeat estimation in fmcw radar via kalman filter tracking. *IEEE Sensors Letters, 4*(5), 1–4.

Banin, L., Schatzberg, U., & Amizur, Y. (2013). Next generation indoor positioning system based on wifi time of flight. In *Proc. 26th int. Tech. Meeting satellite division inst. Navigat.(ION GNSS+)* (pp. 975–982).

Beermann, T. A., Vartapetian, A., Vokac, P., Elmsheuser, J., Barberis, D., Crepe-Renaudin, S. C., et al. (2020). *Implementation of atlas distributed computing monitoring dashboards using influxdb and grafana, Tech. rep., ATL-COM-SOFT-2020-015*.

Brser, C., Kerekes, A., Winter, S., & Leonhardt, S. (2012). Multi-channel optical sensor-array for measuring ballistocardiograms and respiratory activity in bed. In *2012 annual international conference of the IEEE engineering in medicine and biology society* (pp. 5042–5045). IEEE.

Cao, X., Chen, B., & Zhao, Y. (2016). Wi-wri: Fine-grained writing recognition using wi-fi signals. In *2016 IEEE trustcom/BigDataSE/ISPA* (pp. 1366–1373). IEEE.

CDC. (Apr. 2020). *Coronavirus disease 2019 (COVID-19) situation summary*. library Catalog. www.cdc.gov. https://www.cdc.gov/coronavirus/2019-ncov/cases-updates/summary.html.

CDC. (Feb. 2020). *Coronavirus disease 2019 (COVID-19)*. library Catalog. www.cdc.gov. https://www.cdc.gov/coronavirus/2019-ncov/if-you-are-sick/quarantine.html.

Chen, C., Han, Y., Chen, Y., Lai, H.-Q., Zhang, F., Wang, B., et al. (2017). Tr-breath: Time-reversal breathing rate estimation and detection. *IEEE Transactions on Biomedical Engineering, 65*(3), 489–501.

Chowdhury, T. Z., Leung, C., & Miao, C. Y. (2017). Wihacs: Leveraging wifi for human activity classification using ofdm subcarriers' correlation. In *2017 IEEE global conference on signal and information processing (GlobalSIP)* (pp. 338–342). IEEE.

Clemente, J., Valero, M., Li, F., Wang, C., & Song, W. (2020). Helena: Real-time contact-free monitoring of sleep activities and events around the bed. In *IEEE international conference on pervasive computing and communications*.

Davies, L., & Gather, U. (1993). The identification of multiple outliers. *Journal of the American Statistical Association, 88*(423), 782–792.

De Groote, A., Wantier, M., Chéron, G., Estenne, M., & Paiva, M. (1997). Chest wall motion during tidal breathing. *Journal of Applied Physiology, 83*(5), 1531–1537.

Depatla, S., & Mostofi, Y. (2018). Crowd counting through walls using wifi. In *2018 IEEE international conference on pervasive computing and communications (PerCom)* (pp. 1–10). IEEE.

W. J. Dixon, F. J. Massey Jr, Introduction to statistical analysis.

Frey, B. J., & Dueck, D. (2007). Clustering by passing messages between data points. *Science, 315*(5814), 972–976.

Gao, X., Lu, W., Li, F., & Jiang, X. (2013). The application of robust principal component analysis for weak seismic signal enhancement. In *75th EAGE conference & exhibition incorporating SPE EUROPEC 2013* (p. 348). European Association of Geoscientists & Engineers.

Gringoli, F., Schulz, M., Link, J., & Hollick, M. (2019). Free your csi: A channel state information extraction platform for modern wi-fi chipsets. In *Proceedings of the 13th international workshop on wireless network testbeds* (pp. 21–28). Experimental Evaluation & Characterization.

M. A. A. Haseeb, R. Parasuraman, Wisture: Rnn-based learning of wireless signals for gesture recognition in unmodified smartphones, arXiv preprint arXiv: 1707.08569.

Home care for patients with COVID-19 presenting with mild symptoms and management of their contacts, library Catalog. shorturl.at/asAM7 www.who.int.

Huang, C., Wang, Y., Li, X., Ren, L., Zhao, J., Hu, Y., et al. (2020). Clinical features of patients infected with 2019 novel coronavirus in wuhan, China. *The lancet, 395* (10223), 497–506.

J. Humphreys, L. Schoenherr, G. Elia, N. T. Saks, C. Brown, S. Barbour, S. Z. Pantilat, Rapid implementation of inpatient telepalliative medicine consultations during COVID-19 pandemic, journal of pain and symptom ManagementISBN: 0885-3924 publisher: Elsevier.

InfluxDB open source time series database | InfluxDB, library catalog. www.influxdata.com. https://www.influxdata.com/products/influxdb-overview/.

Kaltiokallio, O., Yiğitler, H., Jäntti, R., & Patwari, N. (2014). Non-invasive respiration rate monitoring using a single cots tx-rx pair. In *IPSN-14 proceedings of the 13th international symposium on information processing in sensor networks* (pp. 59–69). IEEE.

Kanso, M. A., & Rabbat, M. G. (2009). Compressed rf tomography for wireless sensor networks: Centralized and decentralized approaches. In *International conference on distributed computing in sensor systems* (pp. 173–186). Springer.

Kay, S. M. (1993). *Fundamentals of statistical signal processing*. Prentice Hall PTR.

Korany, B., Karanam, C. R., Cai, H., & Mostofi, Y. (2019). Xmodal-id: Using wifi for through-wall person identification from candidate video footage. In *The 25th annual international conference on mobile computing and networking* (pp. 1–15).

Li, F., Clemente, J., & Song, W. (2018a). Non-intrusive and non-contact sleep monitoring with seismometer. In *2018 IEEE global conference on signal and information processing (GlobalSIP)* (pp. 449–453). IEEE.

Lindh, W. Q., Pooler, M., Tamparo, C. D., Dahl, B. M., & Morris, J. (2013). *Delmar's comprehensive medical assisting: Administrative and clinical competencies*. Cengage Learning.

Li, F., Song, W., Li, C., & Yang, A. (2019). Non-harmonic analysis based instantaneous heart rate estimation from photoplethysmography. In *ICASSP 2019-2019 IEEE international conference on acoustics, speech and signal processing (ICASSP)* (pp. 1279–1283). IEEE.

Liu, X., Cao, J., Tang, S., Wen, J., & Guo, P. (2015). Contactless respiration monitoring via off-the-shelf wifi devices. *IEEE Transactions on Mobile Computing, 15*(10), 2466–2479.

Liu, X., Cao, J., Tang, S., Wen, J., & Wi-sleep. (2014). Contactless sleep monitoring via wifi signals. In *2014 IEEE real-time systems symposium* (pp. 346–355). IEEE.

Liu, N., Gao, J., Zhang, Z., Jiang, X., & Lv, Q. (2017). High-resolution characterization of geologic structures using the synchrosqueezing transform. *Interpretation, 5*(1), T75–T85.

Liu, N., Li, Z., Sun, F., Li, F., & Gao, J. (2020). Seismic geologic structure characterization using a high-order spectrum-coherence attribute. *Interpretation, 8*(2), T391–T401.

Li, F., Zhang, B., Verma, S., & Marfurt, K. J. (2018b). Seismic signal denoising using thresholded variational mode decomposition. *Exploration Geophysics, 49*(4), 450–461.

Lu, W., & Li, F. (2013). Seismic spectral decomposition using deconvolutive short-time fourier transform spectrogram. *Geophysics, 78*(2), V43–V51.

Lv, S., Lu, Y., Dong, M., Wang, X., Dou, Y., & Zhuang, W. (2017). Qualitative action recognition by wireless radio signals in human–machine systems. *IEEE Transactions on Human-Machine Systems, 47*(6), 789–800.

Maas, D., Wilson, J., & Patwari, N. (2013). Toward a rapidly deployable radio tomographic imaging system for tactical operations. In *38th annual IEEE conference on local computer networks - workshops* (pp. 203–210).

G. K. Nanani, M. Kantipudi, A study of wi-fi based system for moving object detection through the wall, International Journal of Computer Applications 79 (7).

Nandakumar, R., Gollakota, S., & Watson, N. (2015). Contactless sleep apnea detection on smartphones. In *Proceedings of the 13th annual international conference on mobile systems, applications, and services* (pp. 45–57).

S. N. Z. Naqvi, S. Yfantidou, E. Zimányi, Time series databases and influxdb, studienarbeit, université libre de Bruxelles.

Ni, H., Abdulrazak, B., Zhang, D., & Wu, S. (2010). Unobtrusive sleep posture detection for elder-care in smart home. In *International conference on smart homes and health telematics* (pp. 67–75). Springer.

O. o. t. Commissioner. (Mar. 2020). *Coronavirus (COVID-19) update: FDA allows expanded use of devices to monitor patients vital signs remotely, library catalog.* Publisher: FDA. URL shorturl.at/aHPT8 www.fda.gov.

Patwari, N., & Agrawal, P. (2008). Effects of correlated shadowing: Connectivity, localization, and rf tomography. In *2008 international conference on information processing in sensor networks (ipsn 2008)* (pp. 82–93). IEEE.

Patwari, N., Brewer, L., Tate, Q., Kaltiokallio, O., Bocca, M., & Breathfinding. (2014b). A wireless network that monitors and locates breathing in a home. *IEEE Journal of Selected Topics in Signal Processing, 8*(1), 30–42.

Patwari, N., Wilson, J., Ananthanarayanan, S., Kasera, S. K., & Westenskow, D. R. (2014a). Monitoring breathing via signal strength in wireless networks. *IEEE Transactions on Mobile Computing, 13*(8), 1774–1786.

Pulmonary function laboratories: Advice regarding COVID-19, library catalog. www.thoracic.org. https://www.thoracic.org/professionals/clinical-resources/.

Qi, J., Lin, T., Zhao, T., Li, F., & Marfurt, K. (2016). Semisupervised multiattribute seismic facies analysis. *Interpretation, 4*(1), SB91–SB106.

Raj, R., Chen, V., & Lipps, R. (2010). Analysis of radar human gait signatures. *IET Signal Processing, 4*(3), 234–244.

Rao, B. D., & Hari, K. S. (1989). Performance analysis of root-music. *IEEE Transactions on Acoustics, Speech, & Signal Processing, 37*(12), 1939–1949.

Ross, F. (Apr. 2020). *WHOOP investigating respiratory rate pattern and relationship with COVID-19 symptoms*. library Catalog. URL shorturl.at/juwxz) www.ptcommunity.com.

Schmidt, R. (1986). Multiple emitter location and signal parameter estimation. *IEEE Transactions on Antennas and Propagation, 34*(3), 276–280.

Schulz, M., Wegemer, D., & Hollick, M. (2017). Nexmon: Build your own wi-fi testbeds with low-level mac and phy-access using firmware patches on off-the-shelf mobile devices. In *Proceedings of the 11th workshop on wireless network testbeds* (pp. 59–66). Experimental evaluation & CHaracterization.

Sen, S., Lee, J., Kim, K.-H., & Congdon, P. (2013). Avoiding multipath to revive inbuilding wifi localization. In *Proceeding of the 11th annual international conference on Mobile systems, applications, and services* (pp. 249–262).

Shafiq, G., & Veluvolu, K. C. (2014). Surface chest motion decomposition for cardiovascular monitoring. *Scientific Reports, 4*, 5093.

Tahmoush, D., & Silvious, J. (2009). Radar micro-Doppler for long range front-view gait recognition. In *2009 IEEE 3rd international conference on biometrics: Theory, applications, and systems* (pp. 1–6). IEEE.

Tan, S., & Yang, J. (2016). Wifinger: Leveraging commodity wifi for fine-grained finger gesture recognition. In *Proceedings of the 17th ACM international symposium on mobile ad hoc networking and computing* (pp. 201–210).

Tataraidze, A., Olesyuk, R., & Pikhletsky, M. (2019). Can we monitor breathing during sleep via wi-fi on smartphone?. In *2019 41st annual international conference of the IEEE engineering in medicine and biology society (EMBC)* (pp. 6710–6713). IEEE.

Tenhunen, M., Elomaa, E., Sistonen, H., Rauhala, E., & Himanen, S.-L. (2013). Emfit movement sensor in evaluating nocturnal breathing. *Respiratory Physiology & Neurobiology, 187*(2), 183–189. iSBN: 1569-9048 Publisher: Elsevier.

Villasenor, J. D., Belzer, B., & Liao, J. (1995). Wavelet filter evaluation for image compression. *IEEE Transactions on Image Processing, 4*(8), 1053–1060.

Wang, Z., Jiang, K., Hou, Y., Dou, W., Zhang, C., Huang, Z., et al. (2019). A survey on human behavior recognition using channel state information. *IEEE Access, 7*, 155986–156024.

Wang, Y., Liu, J., Chen, Y., Gruteser, M., Yang, J., & Liu, H. (2014). E-eyes: Device-free location-oriented activity identification using fine-grained wifi signatures. In *Proceedings of the 20th annual international conference on Mobile computing and networking* (pp. 617–628).

Wang, W., Liu, A. X., Shahzad, M., Ling, K., & Lu, S. (2017a). Device-free human activity recognition using commercial wifi devices. *IEEE Journal on Selected Areas in Communications, 35*(5), 1118–1131.

Wang, B., Wu, Y., Han, F., Yang, Y.-H., & Liu, K. R. (2011). Green wireless communications: A time-reversal paradigm. *IEEE Journal on Selected Areas in Communications, 29*(8), 1698–1710.

Wang, X., Yang, C., Mao, S., & Phasebeat. (2017b). Exploiting csi phase data for vital sign monitoring with commodity wifi devices. In *2017 IEEE 37th international conference on distributed computing systems (ICDCS)* (pp. 1230–1239). IEEE.

Wang, H., Zhang, D., Ma, J., Wang, Y., Wang, Y., Wu, D., et al. (2016). Human respiration detection with commodity wifi devices: Do user location and body orientation matter?. In *Proceedings of the 2016 ACM international joint conference on pervasive and ubiquitous computing* (pp. 25–36).

F. Wang, F. Zhang, C. Wu, B. Wang, K. R. Liu, Respiration tracking for people counting and recognition, IEEE Internet of Things Journal.

Wang, F., Zhang, F., Wu, C., Wang, B., & Liu, K. R. (2020). Vimo: Vital sign monitoring using commodity millimeter wave radio. In *ICASSP 2020-2020 IEEE international conference on acoustics, speech and signal processing (ICASSP)* (pp. 8304–8308). IEEE.

Wilcoxon, F. (1992). Individual comparisons by ranking methods. In *Breakthroughs in statistics* (pp. 196–202). Springer.

Wilson, J., & Patwari, N. (2010a). See-through walls: Motion tracking using variance-based radio tomography networks. *IEEE Transactions on Mobile Computing, 10*(5), 612–621.

Wilson, J., & Patwari, N. (2010b). Radio tomographic imaging with wireless networks. *IEEE Transactions on Mobile Computing, 9*(5), 621–632.

Wold, S., Esbensen, K., & Geladi, P. (1987). Principal component analysis. *Chemometrics and Intelligent Laboratory Systems, 2*(1–3), 37–52.

Won, M., Zhang, S., & Son, S. H. (2017). Witraffic: Low-cost and non-intrusive traffic monitoring system using wifi. In *2017 26th international conference on computer communication and networks (ICCCN)* (pp. 1–9).

Woyach, K., Puccinelli, D., & Haenggi, M. (2006). Sensorless sensing in wireless networks: Implementation and measurements. In *2006 4th international symposium on modeling and optimization in mobile, ad hoc and wireless networks* (pp. 1–8). IEEE.

Wu, C., Yang, Z., Zhou, Z., Liu, X., Liu, Y., & Cao, J. (2015). Non-invasive detection of moving and stationary human with wifi. *IEEE Journal on Selected Areas in Communications, 33*(11), 2329–2342.

Xiang, P., Ji, P., & Zhang, D. (2018). *Enhance rss-based indoor localization accuracy by leveraging environmental physical features, Wireless Communications and Mobile Computing*.

Xu, Q., Han, Y., Wang, B., Wu, M., & Liu, K. R. (2019). Indoor events monitoring using channel state information time series. *IEEE Internet of Things Journal, 6*(3), 4977–4990.

Yang, H. (2015). Synchrosqueezed wave packet transforms and diffeomorphism based spectral analysis for 1d general mode decompositions. *Applied and Computational Harmonic Analysis, 39*(1), 33–66.

Yang, Y., Cao, J., Liu, X., & Xing, K. (2018b). Multi-person sleeping respiration monitoring with cots wifi devices. In *2018 IEEE 15th international conference on mobile ad hoc and sensor systems (MASS)* (pp. 37–45). IEEE.

Yang, W., Wang, X., Song, A., & Mao, S. (2018a). Wi-wheat: Contact-free wheat moisture detection with commodity wifi. In *2018 IEEE international conference on communications (ICC)* (pp. 1–6). IEEE.

Yang, Z., Zhou, Z., & Liu, Y. (2013). From rssi to csi: Indoor localization via channel response. *ACM Computing Surveys, 46*(2), 1–32.

Youssef, M., Mah, M., & Agrawala, A. (2007). Challenges: Device-free passive localization for wireless environments. In *Proceedings of the 13th annual ACM international conference on Mobile computing and networking* (pp. 222–229).

Zeng, Y., Pathak, P. H., Xu, C., & Mohapatra, P. (2014). Your ap knows how you move: Fine-grained device motion recognition through wifi. In *Proceedings of the 1st ACM workshop on Hot topics in wireless* (pp. 49–54).

Zhang, D., Hu, Y., Chen, Y., & Zeng, B. (2019). Breathtrack: Tracking indoor human breath status via commodity wifi. *IEEE Internet of Things Journal, 6*(2), 3899–3911.

Zhang, D., Ma, J., Chen, Q., & Ni, L. M. (2007). An rf-based system for tracking transceiver-free objects. In *Fifth annual IEEE international conference on pervasive computing and communications (PerCom'07)* (pp. 135–144). IEEE.

Zhang, D., & Ni, L. M. (2009). Dynamic clustering for tracking multiple transceiver-free objects. In *2009 IEEE international conference on pervasive computing and communications* (pp. 1–8). IEEE.

F. Zhang, C. Wu, B. Wang, M. Wu, D. Bugos, H. Zhang, et al, Smars: Sleep monitoring via ambient radio signals, IEEE Transactions on Mobile Computing.

Zhao, Y., & Patwari, N. (2011). Noise reduction for variance-based device-free localization and tracking. In *2011 8th annual IEEE communications society conference on sensor, mesh and ad hoc communications and networks* (pp. 179–187). IEEE.

Zheng, Y., & Men, A. (2012). Through-wall tracking with radio tomography networks using foreground detection. In *2012 IEEE wireless communications and networking conference (WCNC)* (pp. 3278–3283). IEEE.

Zhong, S., Huang, Y., Ruby, R., Wang, L., Qiu, Y.-X., & Wu, K. (2017). Wi-fire: Device-free fire detection using wifi networks. In *2017 IEEE international conference on communications (ICC)* (pp. 1–6). IEEE.

Zhou, Q., Wu, C., Xing, J., Li, J., Yang, Z., & Yang, Q. (2017). Wi-dog: Monitoring school violence with commodity wifi devices. In *International conference on wireless algorithms, systems, and applications* (pp. 47–59). Springer.

F. Zhou, T. Yu, R. Du, G. Fan, Y. Liu, Z. Liu, J. Xiang, Y. Wang, B. Song, X. Gu, Clinical course and risk factors for mortality of adult inpatients with COVID-19 in wuhan, China: A retrospective cohort study, the lancet ISBN: 0140-6736 Publisher: Elsevier.

Zhu, Y., Zhu, Y., Zhao, B. Y., & Zheng, H. (2015). Reusing 60ghz radios for mobile radar imaging. In *Proceedings of the 21st annual international conference on mobile computing and networking* (pp. 103–116).

Zou, M., Wang, C., Li, F., & Song, W. (2018). Network phenotyping for network traffic classification and anomaly detection. In *2018 IEEE international symposium on technologies for homeland security (HST)* (pp. 1–6). IEEE.

Zou, Y., Wang, Y., Ye, S., Wu, K., & Ni, L. M. (2017). Tagfree: Passive object differentiation via physical layer radiometric signatures. In *2017 IEEE international conference on pervasive computing and communications (PerCom)* (pp. 237–246). IEEE.